# Supporting information

## Efficient synthesis of isosorbide-based polycarbonate with scalable dicationic ionic liquid catalysts by balancing the reactivity of the endo-OH and exo-OH

Weiwei Wang [a,b], Yaqin Zhang [a], Zifeng Yang [a,b], Zhencai Zhang [b], Wenjuan Fang [a], Donghui Niu [a], Hongyan He [a,b,c] and Fei Xu *[a,b,c,d]

[a] CAS Key Laboratory of Green Process and Engineering, State Key Laboratory of Multiphase Complex Systems, Beijing Key Laboratory of Ionic Liquids Clean Process, Institute of Process Engineering, Chinese Academy of Sciences, Beijing 100190, China.

[b] School of Chemical Engineering, University of Chinese Academy of Sciences, Beijing 100049, China.

[c] Dalian National Laboratory for Clean Energy, Dalian 116023, China.

[d] Zhongke Langfang Institute of Process Engineering, Langfang 065001, China.

*Corresponding E-mail: fxu@ ipe.ac.cn*

## 1. Synthesis and characterization of DILs

Bis-(3-methyl-1-imidazole)-ethylene diiodide

1-Methylimidazole (0.06 mol) and 1,2-diiodoethane (0.03 mol) were weighed into a 50ml one-necked flask, 40ml tetrahydrofuran was added as a solvent, and kept stirring at room temperature for 2 weeks. Then, pure bis-(3-methyl-1-imidazole)-ethylene diiodized ($[C_2(Min)_2][I]_2$) was obtained after filtration, washing and drying.[1]

Bis-(3-methyl-1-imidazole)-ethylene dichloride

1-Methylimidazole (0.008 mol) and 1,2-diiodoethane (0.004 mol) were weighed into a 15-mL Ace pressure tube, and then the mixture was heated to 130°C kept stirring for 12h. Finally, pure bis-(3-methyl-1-imidazole)-ethylene dichloride ($[C_2(Min)_2][Cl]_2$) was obtained after filtration, washing and drying.[2]

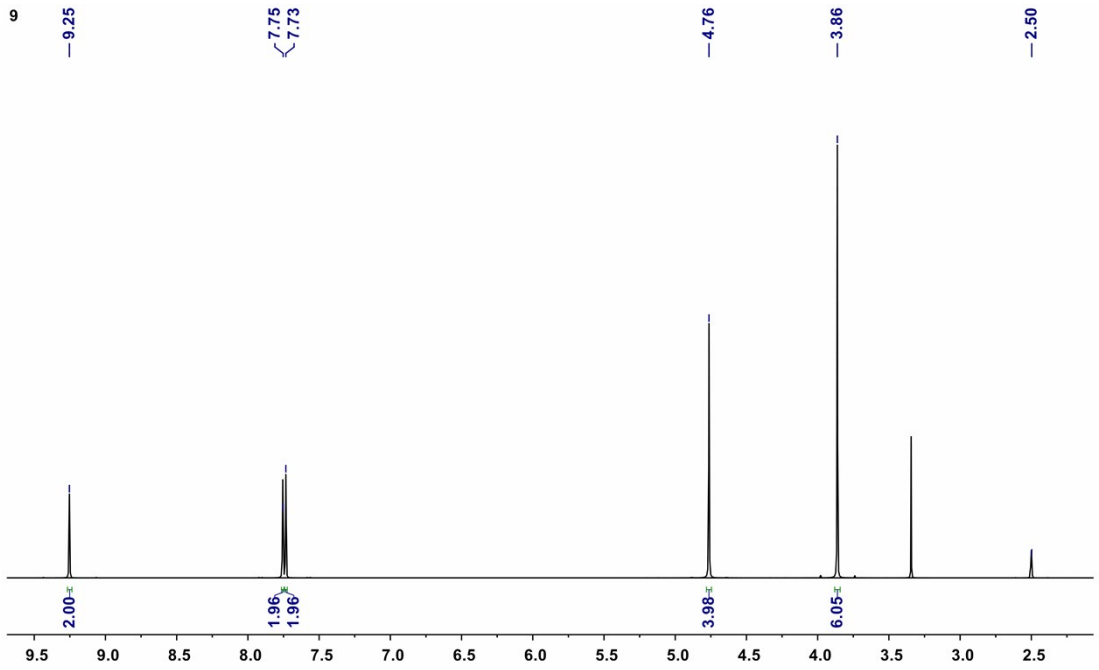


**Fig. S1.** $^{1}$H NMR of $[C_2(Min)_2][Br]_2$ ($d_6$-DMSO, 600 MHz).

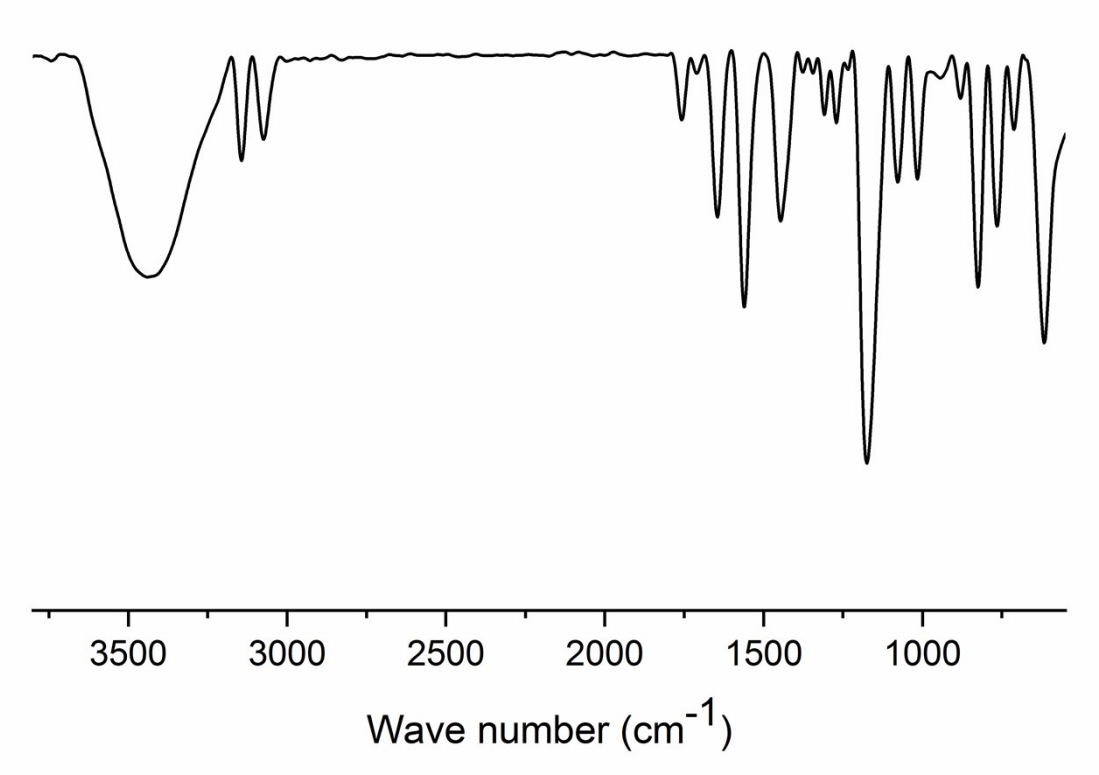


**Fig. S2.** Fourier Infrared spectroscopy of $[C_2(Min)_2][Br]_2$ (KBr).

$^{1}$H NMR (($d_6$-DMSO, 600 MHz) δ 9.21 (s, 2H), 7.74 (s, 2H), 7.71 (s, 2H), 4.75 (s, 4H), 3.86 (s, 6H). FT-IR (KBr, cm$^{-1}$) :3435, 3145, 3015, 1753, 1647, 1557, 1445, 1175, 619.

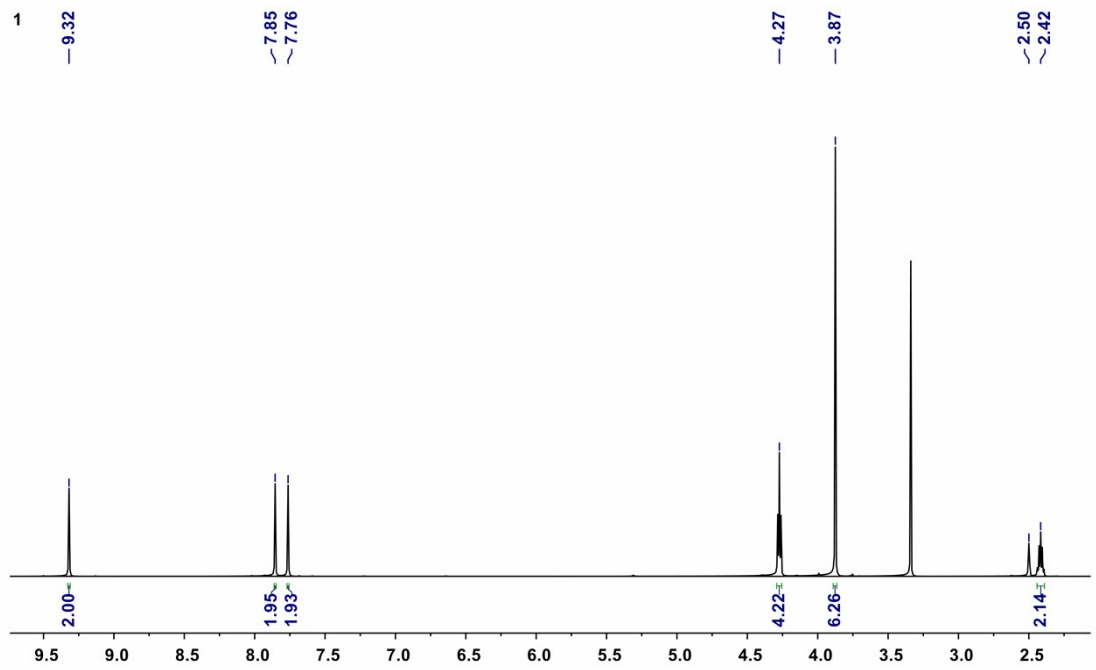


**Fig. S3.** 1H NMR of $[C_3(Min)_2][Br]_2$ ($d_6$-DMSO, 600 MHz).

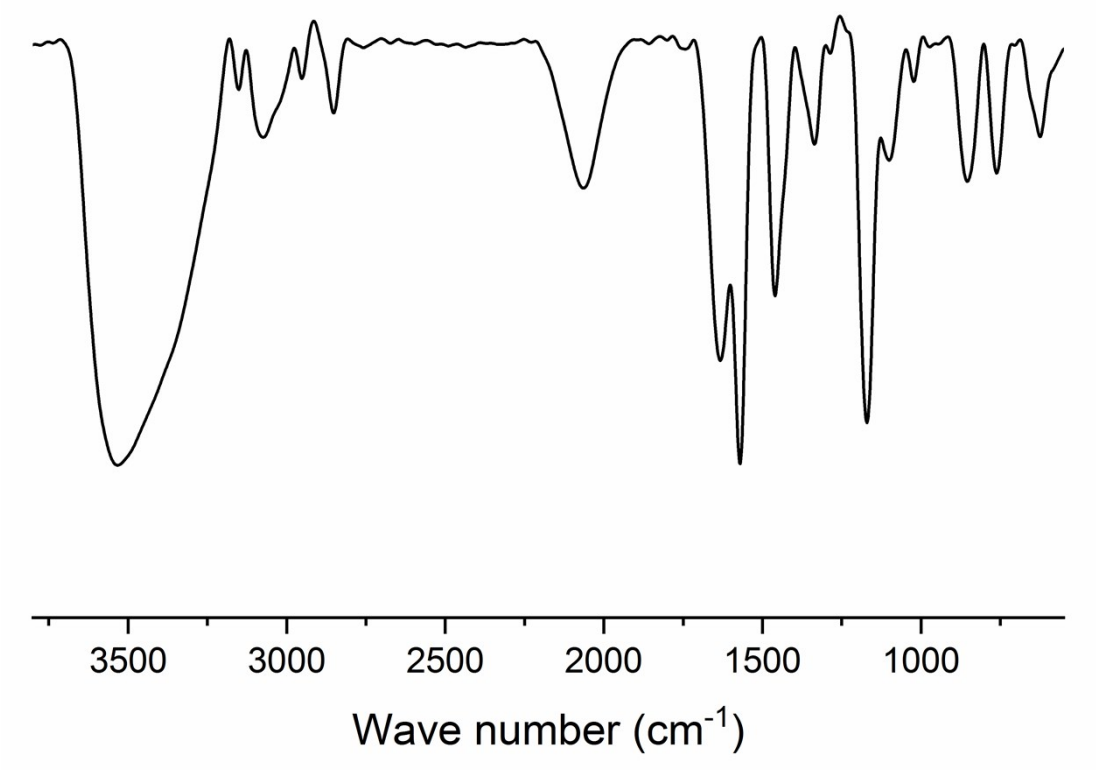


**Fig. S4.** Fourier Infrared spectroscopy of $[C_3(Min)_2][Br]_2$ (KBr).

$^1$H NMR ($d_6$-DMSO, 600 MHz) δ 9.32 (s, 2H), 7.85 (s, 2H), 7.76 (s, 2H), 4.27 (s, 4H), 3.87 (s, 6H), 2.42 (s, 2H). FT-IR (KBr, cm$^{-1}$) :3536, 3150, 3078, 2945, 2853, 1634, 1569, 1460, 1163, 624.

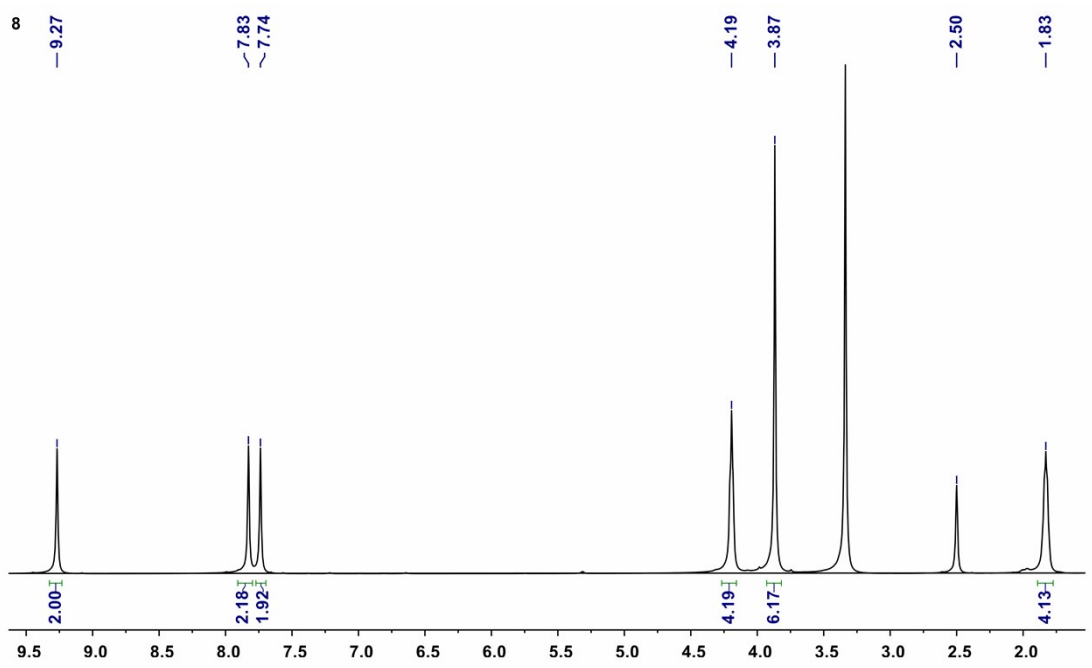


**Fig. S5.** 1H NMR of $[C_4(Min)_2][Br]_2$ ($d_6$-DMSO, 600 MHz).

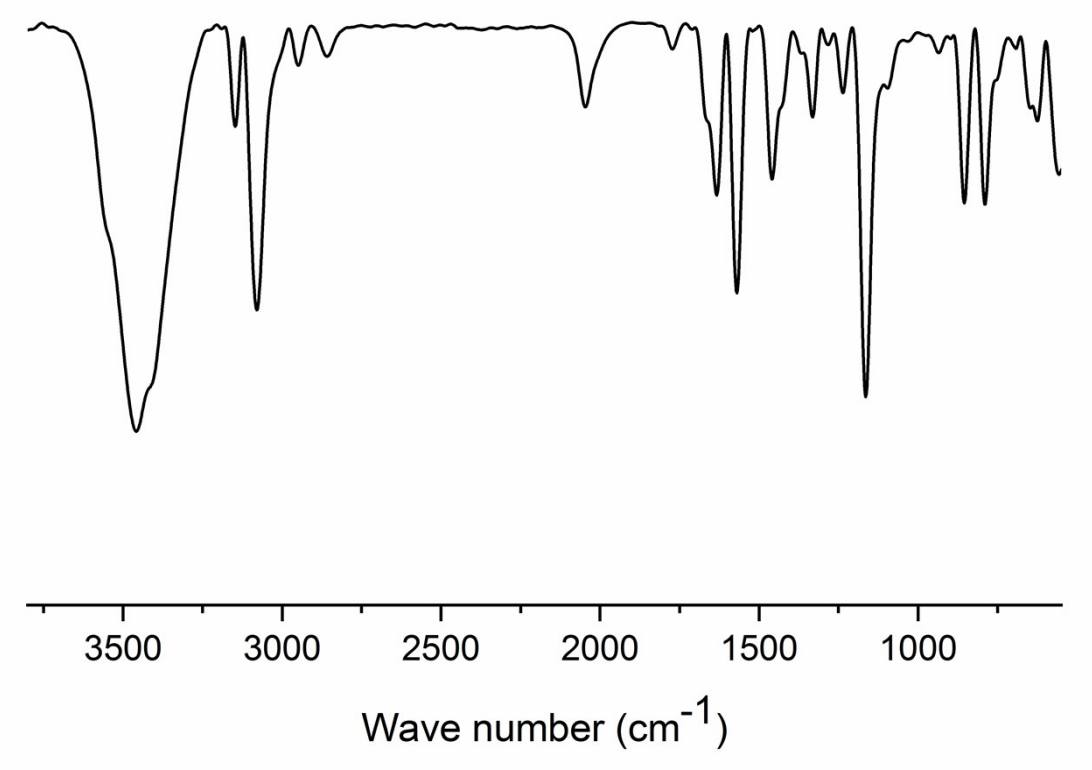


**Fig. S6.** Fourier Infrared spectroscopy of $[C_4(Min)_2][Br]_2$ (KBr).

$^1$H NMR ($d_6$-DMSO, 600 MHz) δ 9.27 (s, 2H), 7.83 (s, 2H), 7.74 (s, 2H), 4.19 (s, 4H), 3.87 (s, 6H), 1.83 (s, 4H). FT-IR (KBr, cm$^{-1}$) : 3454, 3150, 3082, 2945, 2858, 1632, 1572, 1455, 619.

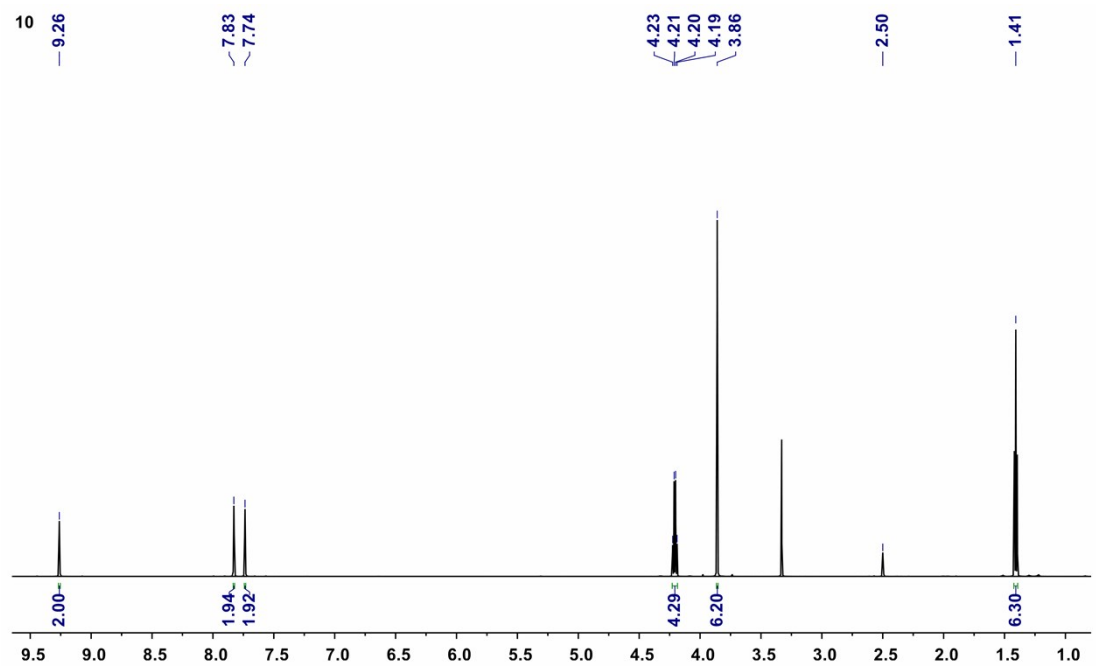


**Figure S7.** 1H NMR of $[C_5 (Min)_2][Br]_2$ ($d_6$-DMSO, 600 MHz).

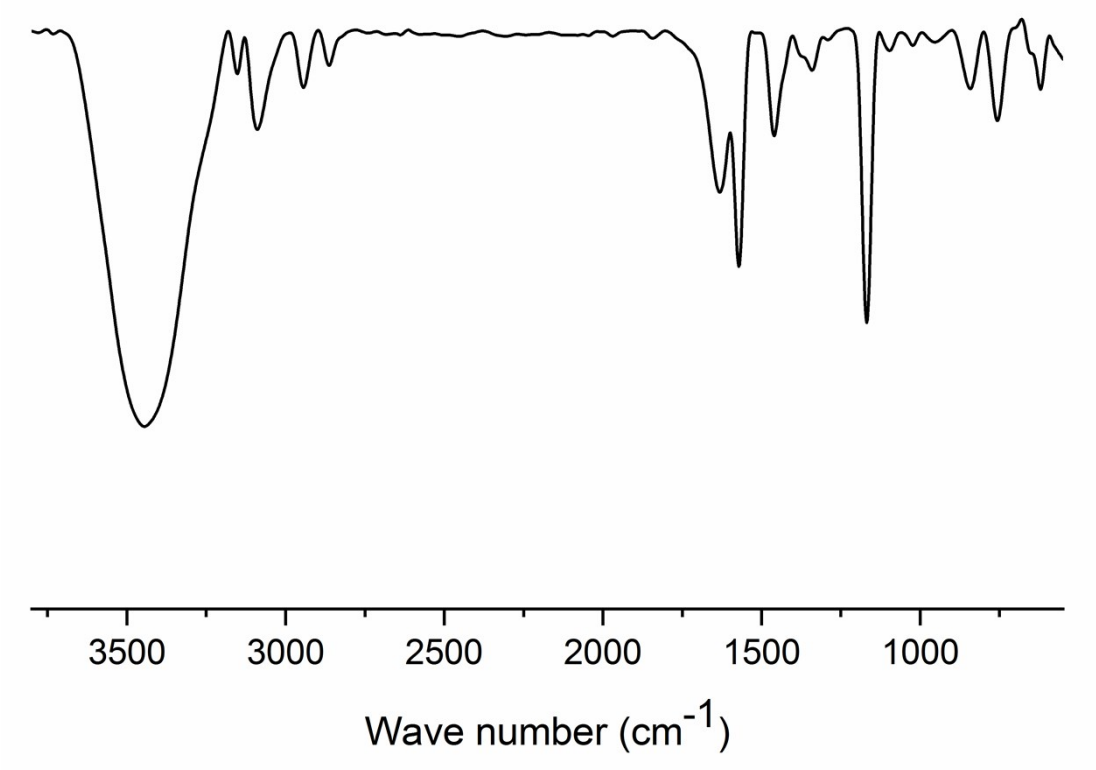


**Fig. S8.** Fourier Infrared spectroscopy of $[C_5 (Min)_2][Br]_2$.

$^1$H NMR ($d_6$-DMSO, 600 MHz) δ 9.26 (s, 2H), 7.83 (t, $J$ = 1.7 Hz, 2H), 7.74 (t, $J$ = 1.7 Hz, 2H), 4.20 (t, $J$ = 7.3 Hz, 4H), 3.86 (s, 6H), 1.41 (t, $J$ = 7.3 Hz, 6H). FT-IR (KBr, cm$^{-1}$) :3447, 3155, 3085, 2940, 2861, 1634, 1574, 1459, 1168, 622.

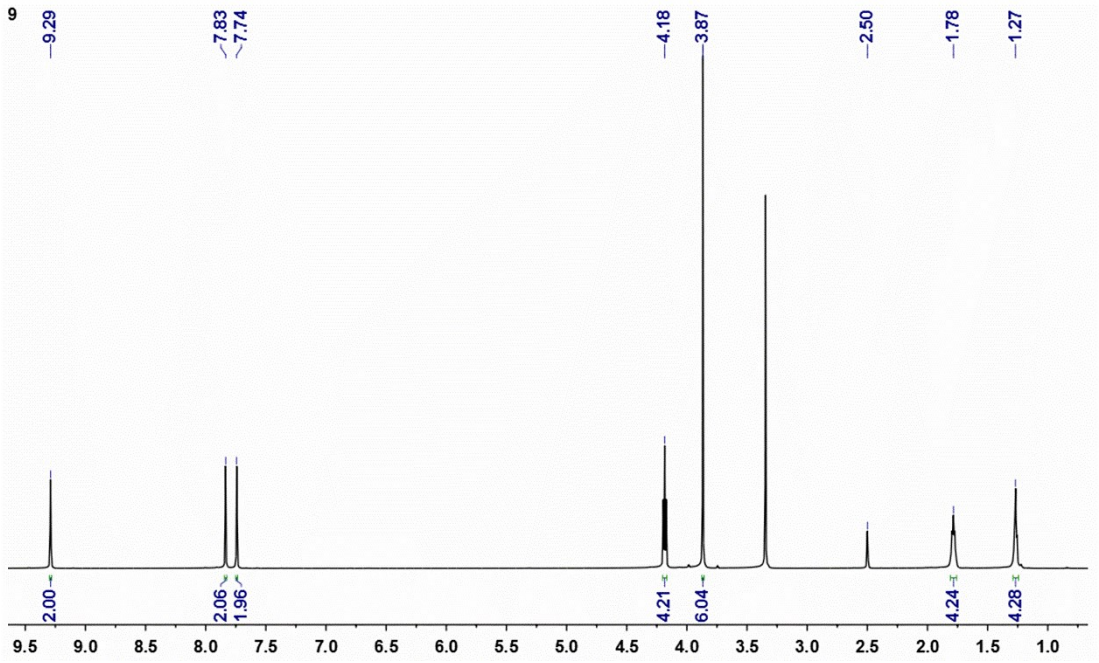


**Fig. S9.** $^{1}$H NMR of $[C_6 (Min)_2][Br]_2$ ($d_6$-DMSO, 600 MHz).

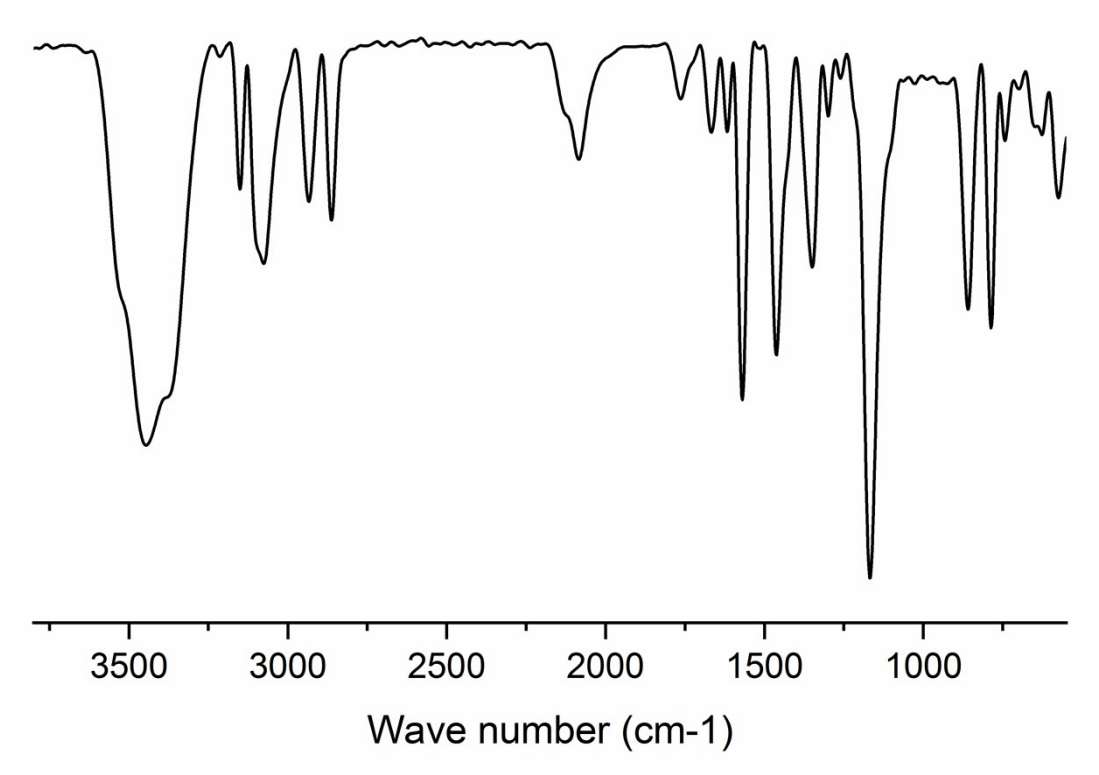


**Fig. S10.** Fourier Infrared spectroscopy of $[C_6(Min)_2][Br]_2$ (KBr).

$^{1}$H NMR ($d_6$-DMSO, 600 MHz) δ 9.29 (s, 2H), 7.83 (s, 2H), 7.74 (s, 2H), 4.18 (s, 4H), 3.87 (s, 6H), 1.78 (s, 4H), 1.27 (s, 4H). FT-IR (KBr, $cm^{-1}$) :3446, 3147, 3078, 2935, 2858, 1669, 1614, 1567, 1173, 629.

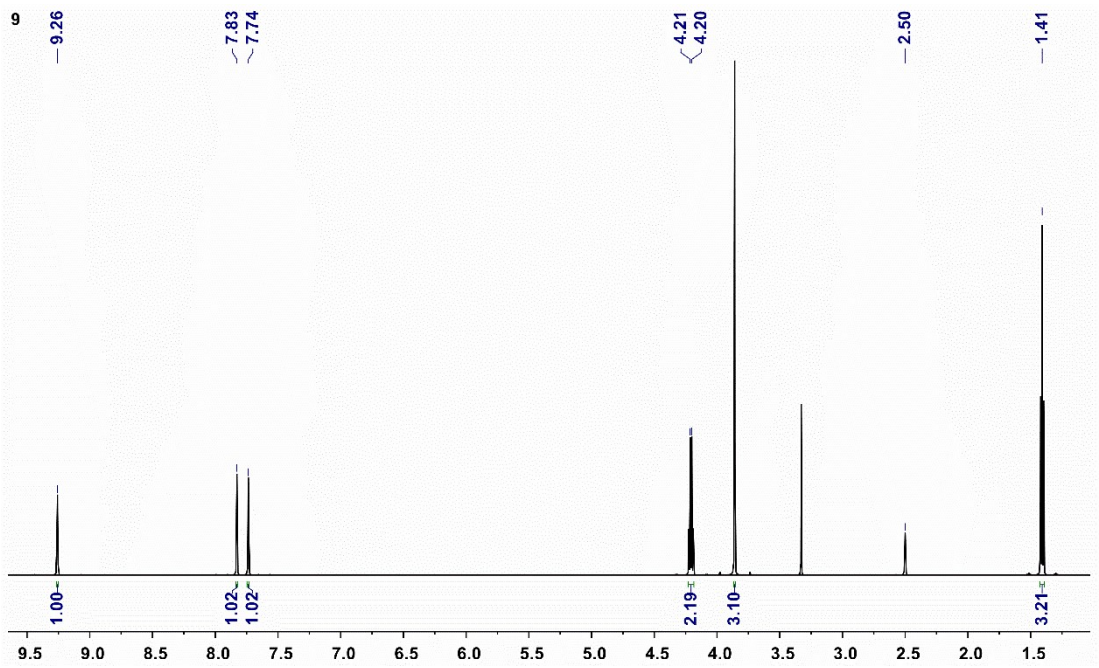


**Fig. S11.** $^{1}$H NMR of [Emin]Br ($d_6$-DMSO, 600 MHz).

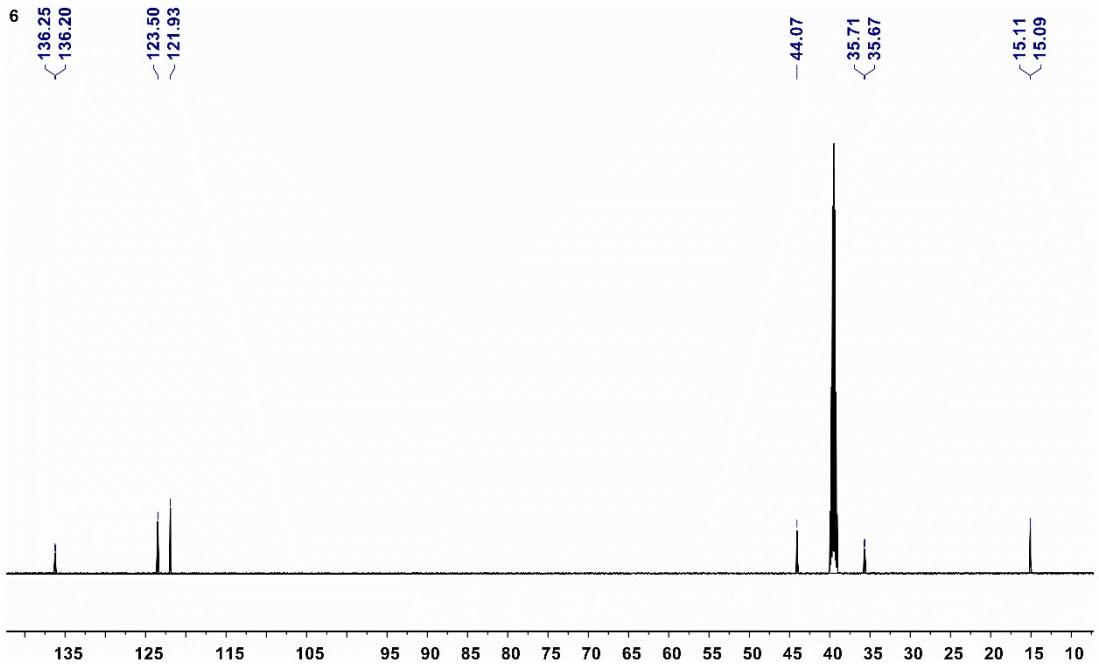


**Fig. S12.** $^{13}$C NMR of [Emin]Br ($d_6$-DMSO, 150 MHz).

$^{1}$H NMR ($d_6$-DMSO, 600 MHz) δ 9.26 (s, 1H), 7.83 (t, $J$ = 1.7 Hz, 1H), 7.74 (t, $J$ = 1.7 Hz, 1H), 4.21 (q, $J$ = 7.3 Hz, 2H), 3.86 (s, 3H), 1.41 (t, $J$ = 7.3 Hz, 3H). $^{13}$C NMR ($d_6$-DMSO, 150 MHz) δ 136.23 (d, $J$ = 6.9 Hz), 123.50 (s), 121.93 (s), 44.07 (s), 35.69 (d, $J$ = 6.8 Hz).

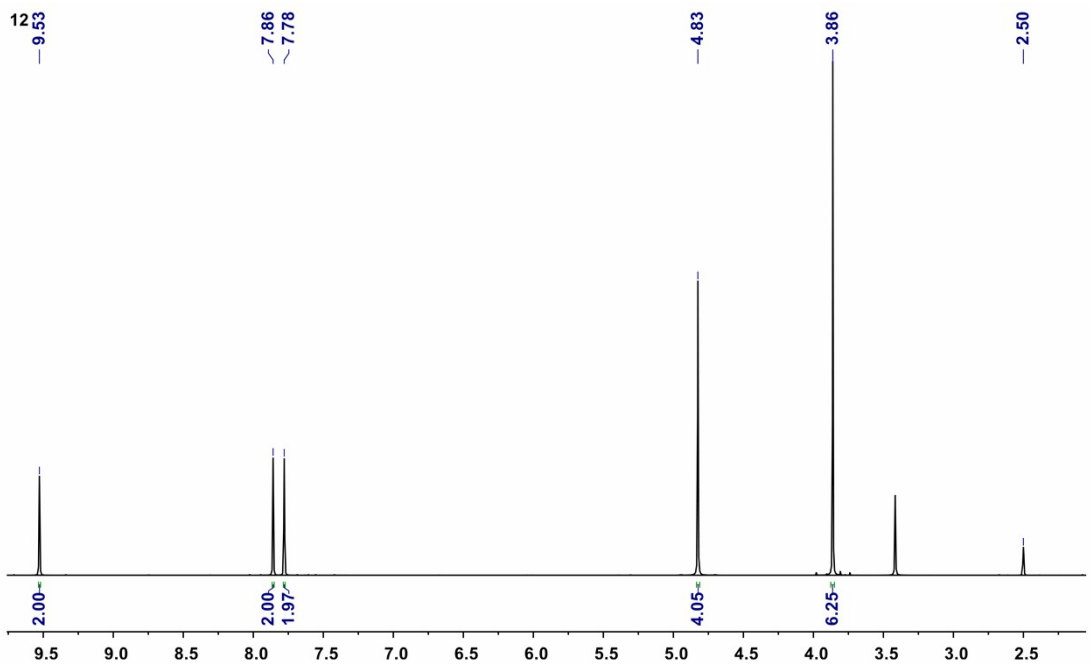


**Fig. S13.** $^{1}$H NMR of $[C_2(Min)_2][Cl]_2$ ($d_6$-DMSO, 600 MHz).

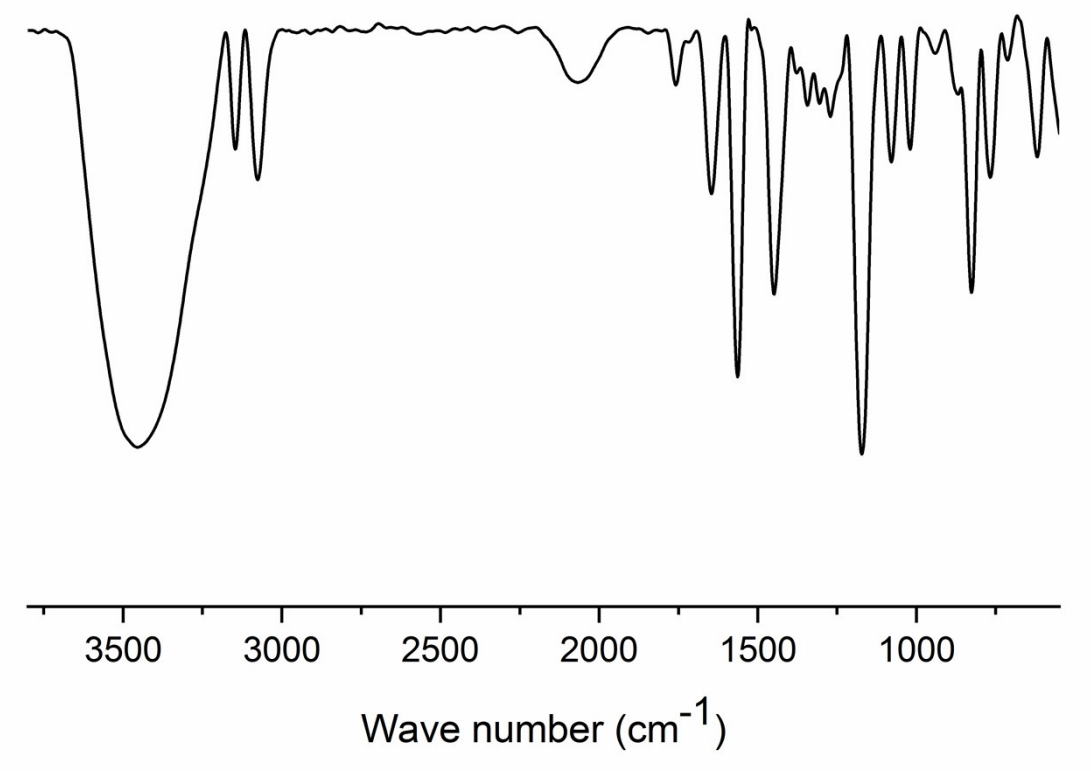


**Fig. S14.** Fourier Infrared spectroscopy of $[C_2(Min)_2][Cl]_2$ (KBr).

$^{1}$H NMR ($d_6$-DMSO, 600 MHz) δ 9.53 (s, 2H), 7.86 (s, 2H), 7.78 (s, 2H), 4.83 (s, 4H), 3.86 (s, 6H). FT-IR (KBr, cm$^{-1}$) :3454, 3142, 3073, 1756, 1647, 1562, 1173, 624.

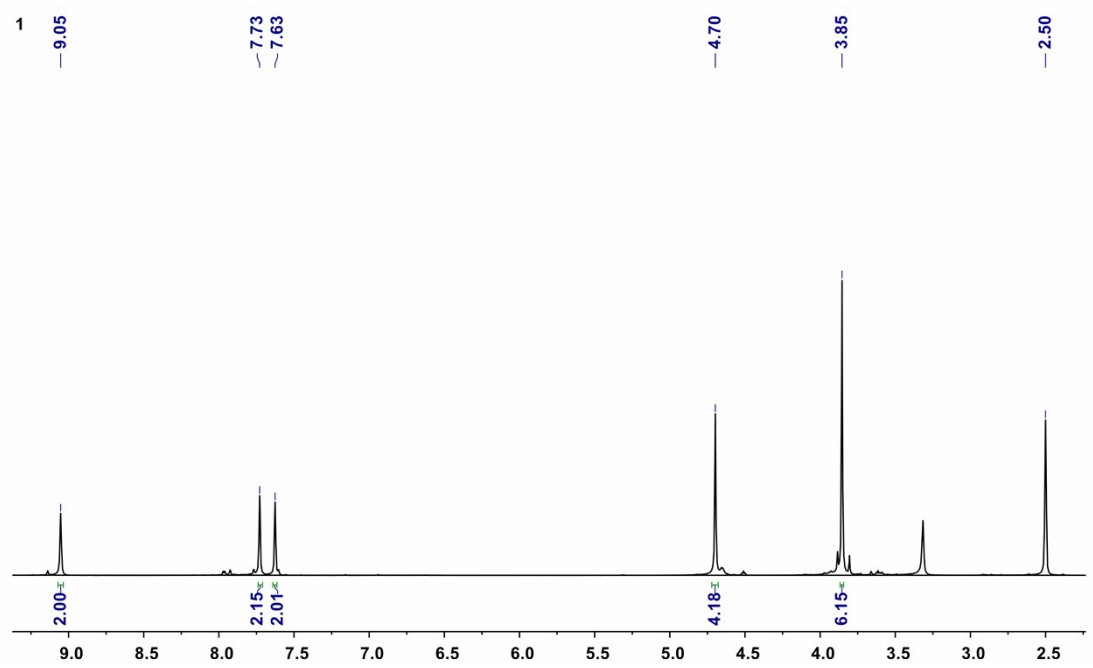


**Fig. S15.** $^{1}$H NMR of $[C_2(Min)_2][I]_2$ ($d_6$-DMSO, 600 MHz).

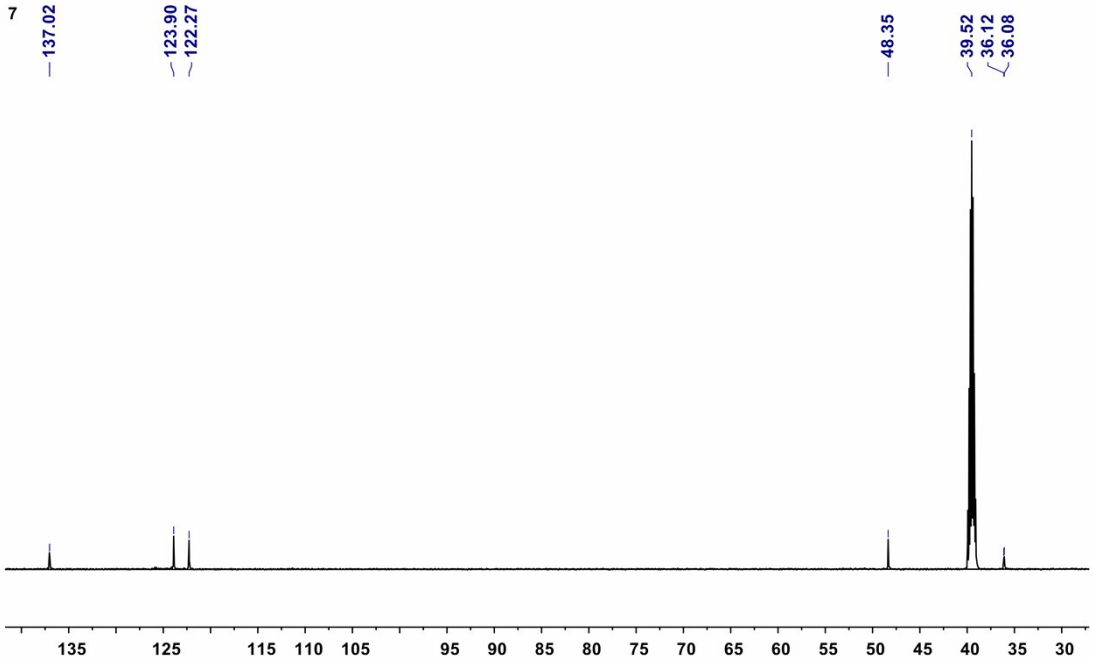


**Fig. S16.** $^{13}$C NMR of $[C_2(Min)_2][I]_2$ (DMSO 150MHZ).

$^{1}$H NMR ($d_6$-DMSO, 600 MHz) δ 9.05 (s, 2H), 7.73 (s, 2H), 7.63 (s, 2H), 4.70 (s, 4H), 3.85 (s, 6H). $^{13}$C NMR ($d_6$-DMSO, 150 MHz) δ 136.23 (d, $J$ = 6.9 Hz), 123.50 (s), 121.93 (s), 44.07 (s), 35.69 (d, $J$ = 6.8 Hz).

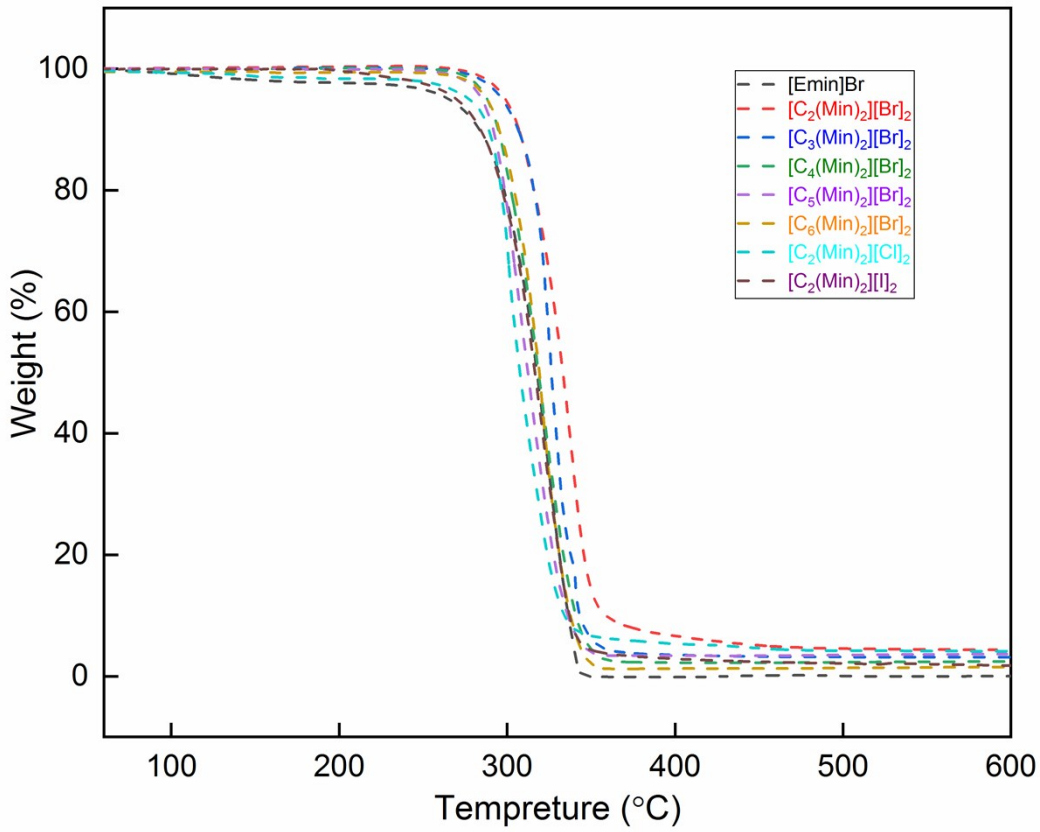


**Fig. S17.** TGA curve of different catalysts.

**Table S1.** Thermal decomposition temperature of catalysts. [a]

| Entry | Catalyst | $T_{d\text{-}5\%}$ [b] (°C) | $T_{d\text{-}max}$ [c] (°C) |
|---|---|---|---|
| 1 | [Emin][Br] | 255 | 325 |
| 2 | $[C_2(Min)_2][Br]_2$ | 300 | 339 |
| 3 | $[C_3(Min)_2][Br]_2$ | 297 | 326 |
| 4 | $[C_4(Min)_2][Br]_2$ | 288 | 320 |
| 5 | $[C_5(Min)_2][Br]_2$ | 285 | 312 |
| 6 | $[C_6(Min)_2][Br]_2$ | 288 | 320 |
| 7 | $[C_2(Min)_2][Cl]_2$ | 278 | 305 |
| 8 | $[C_2(Min)_2][I]_2$ | 269 | 322 |

[a] Measured by TGA at nitrogen atmosphere.

[b] Temperature at 5% weight loss ($T_{d\text{-}5\%}$).

[c] Temperature at maximum weight loss rate.

**2. Research on transesterification kinetics**

Determination of the concentration of phenol

The standard curve of phenol content was determined by the concentration of phenol and the corresponding peak area under the specified conditions (elution with a 50/50 initial ratio of acetonitrile/water, injection volume was 20 μL, the test temperature was 40 °C)

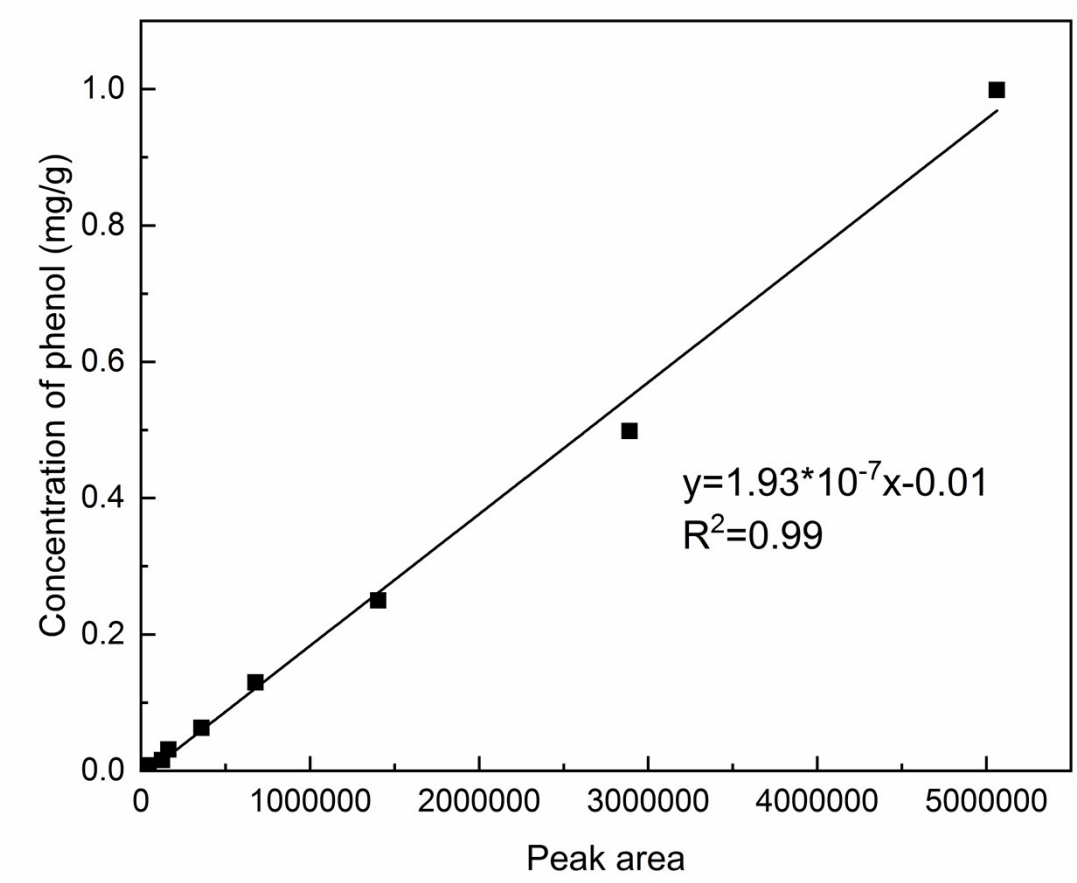


**Fig.** S18 Relationship between phenol concentration and peak area

### 3. Kinetic study on different transesterification temperature

The reaction temperature had a direct effect on the reversible transesterification reaction rate and the conversion rate of raw materials. Since the transesterification process between DPC and ISO was considered a secondary reaction, the following equation was used to calculate the forward reaction rate and equilibrium constant.[3-5]

$k^{+}t=[P]/([A_0]_2-[P][A_0])$

$k=k+/[Cat.]$

$K=[P]_{eq}^{2}/([A_0]_2-[P]_{eq}[A_0])^2$

where $k^{+}$ represents the forward reaction rate constant; the reaction time is expressed by t; [P] is the concentration of phenol; k is the forward reaction rate; [Cat.] refers to the concentration of the catalyst, which is a constant; $[A_0]$ is the initial concentration of the functional groups; K is the equilibrium reaction rate constant; $[P]_{eq}$ is the molar concentration of phenol at equilibrium.

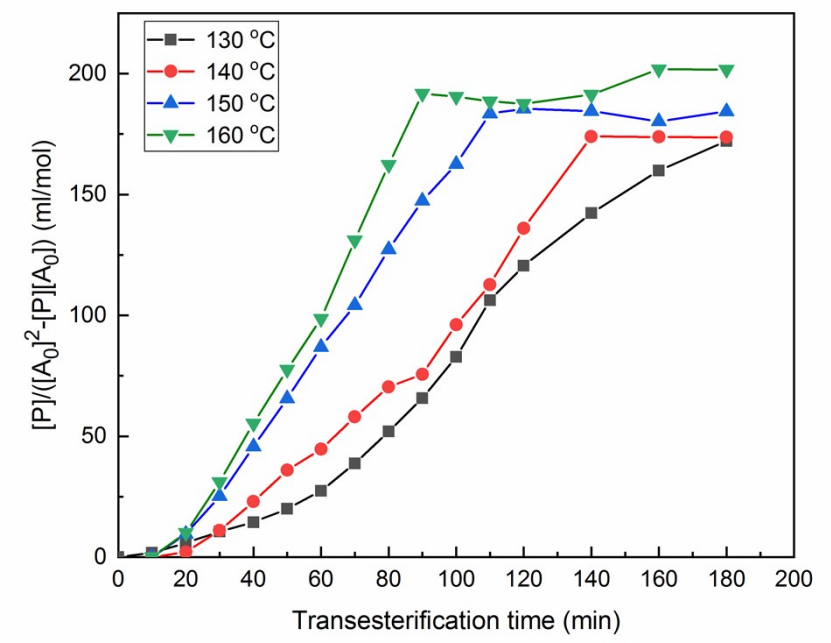


**Fig. S19** Kinetic curve of transesterification at different temperatures.

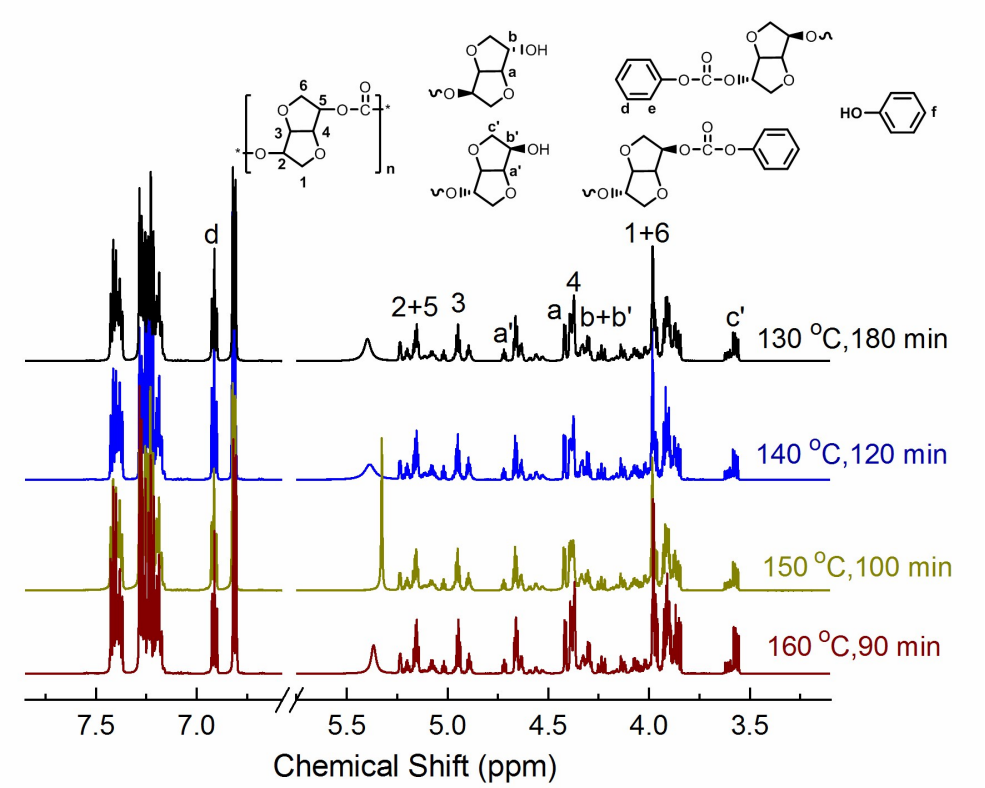


**Fig. S20** Structure comparison of oligomers under different transesterification conditions.

## 4. Catalyst mechanism

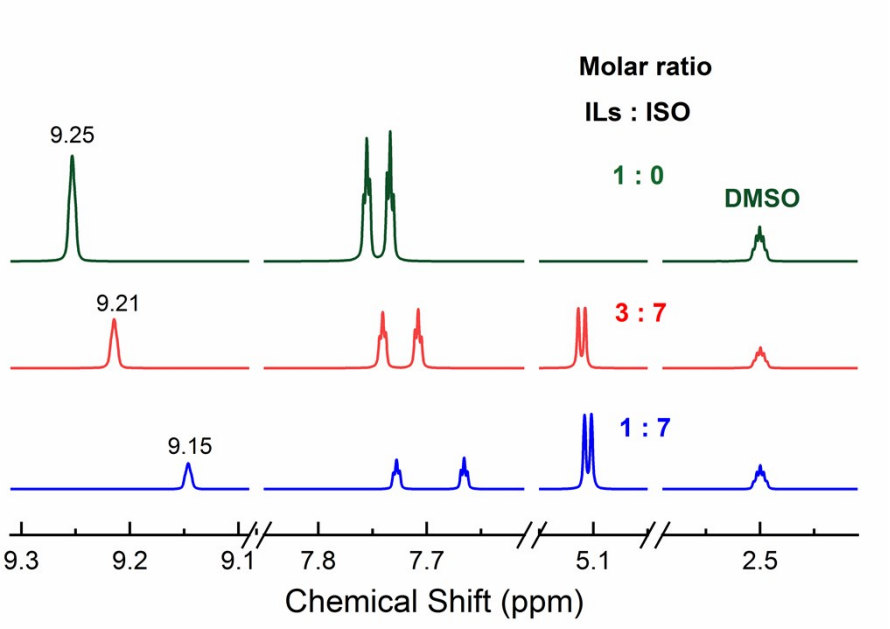


**Fig. S21.** $^{1}$H NMR of $[C_2(Min)_2][Br]_2$ after mixing with ISO.

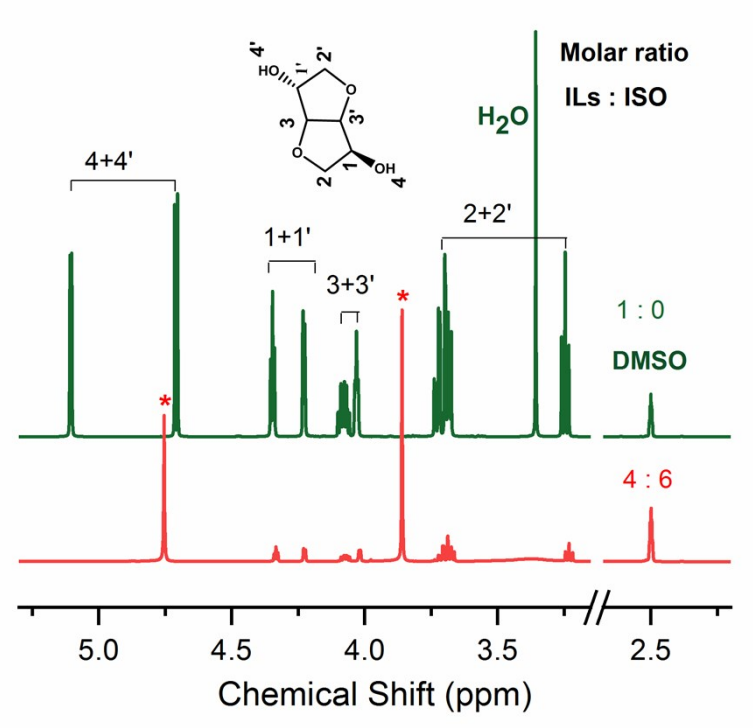


**Fig. S22.** $^{1}$H NMR of ISO after mixing with $[C_2(Min)_2][Br]_2$.

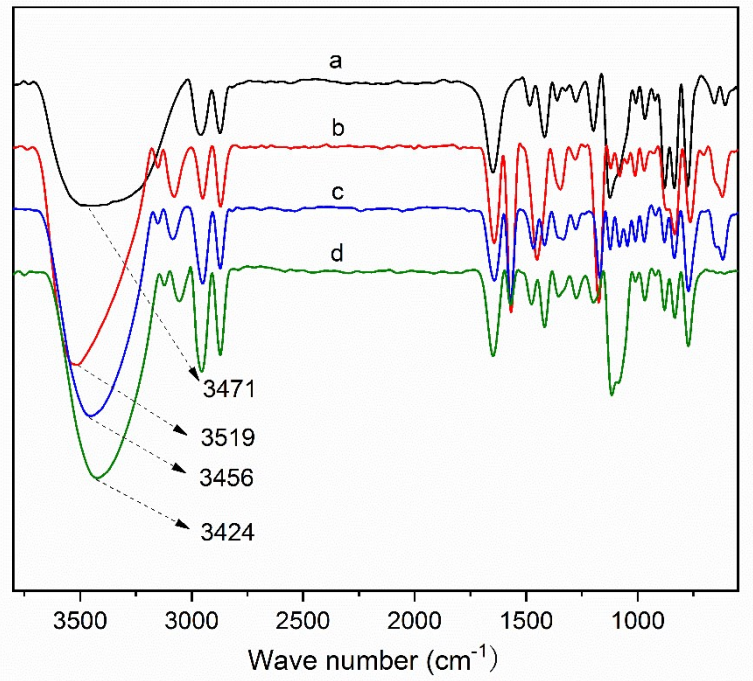


**Fig. S23.** Fourier Infrared Spectroscopy of ISO (a), $[C_2(Min)_2][Cl]_2$ and ISO (b), $[C_2(Min)_2][Br]_2$ and ISO (c), $[C_2(Min)_2][I]_2$ and ISO (d).

## References


1. C. Cao, Y. Zhuang, J. Zhao, H. Liu, P. Geng, G. Pang and Y. Shi, *Synthetic Communications*, 2011, **42**, 380-387.
2. M. Lee, Y.-H. Lee, J. H. Park and U. H. Choi, *Organic Electronics*, 2017, **48**, 241-247.
3. M. Zhang, Y. Tu, Z. Zhou and G. Wu, *Polymer Chemistry*, 2020, **11**, 5512-5525.
4. C. Ma, F. Xu, W. Cheng, X. Tan, Q. Su and S. Zhang, *ACS Sustainable Chemistry & Engineering*, 2018, **6**, 2684-2693.
5. F. L. Bi, Z. H. Xi, L. Zhao, *Int. J. Chem. Kinet.* 2018, **50**, 188-203.